

Long Term Stability of the Upgraded Tevatron BPMs

Rob Kutschke, CD/CEPA

Abstract

This note uses techniques developed in Beams-doc-1925 to set an upper limit on the stability of the upgraded Tevatron BPM system over a period of about 19 weeks. The stability of the proton position measurement is demonstrated to be $< 40 \mu\text{m}$ for a typical BPM and $< 80 \mu\text{m}$ for the worst case BPM. Excluding two anomalous BPMs, the stability of the anti-proton position measurement is demonstrated to be $< 60 \mu\text{m}$ for a typical BPM and $< 150 \mu\text{m}$ for the worst case BPM. The two anomalous BPMs show jumps in the anti-proton position that appear to be instrumental effects; the properties of these jumps are recorded in this note. The cause of these jumps is currently under investigation.

1 Introduction

The requirements document for the Tevatron BPM Upgrade, Beams-doc-554-v3, states in Table 2 that the required long term stability of the BPM system should be $< 20 \mu\text{m}$. One of the challenges when assessing the long term stability of the upgraded Tevatron BPMs is to find a reference quantity that is, itself, sufficiently stable. Beams-doc-1925 Figure 6 shows that the measured size of the helix is remarkably stable, of order $40 \mu\text{m}$ for protons and $50 \mu\text{m}$ for anti-protons for the six weeks included in that study. This stability was achieved even though the central orbit changed by 1 or 2 mm over the course of that study (Beams-doc-1925, Figure 7). The measured size of the helix includes contributions from both true beam motion and instrumental effects. Therefore the quoted number represents an upper bound on the stability of the instrument. While this does not prove the requirement of $< 20 \mu\text{m}$, it is the best demonstration yet for the long term stability of the system. This information was present in the figures in Beams-doc-1925 but its significance was not emphasized in the text.

The main purpose of this document is to point out that the stability of the helix size measurements is the best measure we have yet found to establish the long term stability of the position measurements. The document also extends the study from six weeks to about 19 weeks. In addition, this document studies two BPMs that have unexplained jumps in the anti-proton helix size.

The data discussed in this note were taken at the start of each store by Mike Martens' program that determines the cancellation coefficients. His program

mailed me a copy of the data set for each store and I processed the data offline. The data include 93 HEP stores from June 18, 2005 to October 31, 2005, inclusive. A few stores from this period were not included in this analysis.¹

The notation used in this note were originally defined in Beams-doc-1863,

p_C The measured proton position on the central orbit.

p_H The measured proton position when the helix is open.

\bar{p}_H The measured anti-proton position when the helix is open.

The quantity $p_H - p_C$ measures the size of the proton helix and the quantity $\bar{p}_H - p_C$ measures the size of the anti-proton helix.

A total of 217 of the 236 BPMs were included in this study. Some BPMs were skipped because the anti-proton cables were not connected and others were skipped because the anti-proton data was unreliable. The anti-proton data is unreliable when the size of the proton helix is too small, which gives too short a lever arm to determine the cancellation coefficients. In this study, a BPM was included only if both proton and anti-proton data were available.

On a few stores, there were a handful of BPMs for which the position was recorded as 999.0 mm, which indicates that the BPM sum signal was below threshold. There were also a handful of cases for which the proton position was recorded as 0.0 mm, which indicates that the house believes it is still waiting for the first injection. I have not tried to track down why these rare cases occur. In these cases, the offending BPMs were dropped but remaining good data from the store were included in the analysis.

2 Typical Time Series Data

Figure 1 shows typical data from this study. The upper plot shows the measured size of the proton helix, $p_H - p_C$, at HA32 measured once per store for all stores in this study; the RMS spread of these 91 data points is $R_p = 39 \mu\text{m}$. The second plot shows the size of the anti-proton helix, $\bar{p}_H - p_C$, at HA32; the RMS spread of these data points is $R_{\bar{p}} = 62 \mu\text{m}$. The bottom two plots show the same information for VA33, for which $R_p = 38 \mu\text{m}$ and $R_{\bar{p}} = 64 \mu\text{m}$.

3 Long Term Stability of the Helix Sizes

The above procedure was repeated to determine R_p and $R_{\bar{p}}$ for each of the 217 BPMs in this study². The top plot in Figure 2 shows a histogram of R_p ; there

¹Two stores produced data that gave read errors and, on a few stores, it appeared that the anti-protons were never injected; in the latter cases, a good store followed quickly afterwards and the good store was included in this study.

²Some BPMs have a proton helix size that is very close to the cut that delimits the unreliable anti-proton data. For these BPMs, if at least 2/3 of the stores passed the cut, the BPM was retained in the study; the RMS was computed using only the stores that passed the cut.

is one entry for each of the 217 BPMs in the study. There are no outliers and all of the entries are tightly clustered between about 15 and 80 μm , with a mean value of 40 μm . This indicates that both the helix size, and its measurement, are remarkably stable over a period of 19 weeks, even though the central orbit has moved by several mm during this time.

The lower plot in Figure 2 shows a histogram of $R_{\bar{p}}$ with one entry from each of the 217 BPMs. In contrast with the upper histogram, there are definite outliers, including one data point in the overflow; these will be discussed in the following section. The main body of the anti-proton data is more spread out than is the proton data, with a mean value of 62 μm and a worst case, not including the outliers, of about 150 μm ; the following section will show that the two points near 150 μm indeed belong in the tail of the main body of the data. The broader distribution not surprising because it is necessary to subtract the proton contamination on the anti-proton cables before computing the anti-proton position, which introduces some smearing.

4 Study of the Outliers

All four BPMs with $R_{\bar{p}} > 0.12$ mm (red and magenta) were initially classified as outliers and were selected for further study. For reference, four BPMs from the tail, those with $0.1 \leq \text{RMS} < 0.12$ (green), were also included. Figure 3 shows the time series of the anti-proton helix size for each of these eight BPMs. For each BPM, the size of the proton helix, $p_H - p_C$, is noted in the figure caption; recall that the cut that defines unreliable anti-proton data is $|p_H - p_C| < 0.25$ mm. The features of these data are:

- The most striking feature is the large step in the measured anti-proton helix size for VA14. For this BPM $|p_H - p_C| \gg 0.25$, so the anti-proton data should be among the most reliable. The step is definitely present but one cannot tell from this data alone if it is true beam motion or an instrumental artifact.
- The next most striking feature is the data for HD12, which shows several steps between stores 56 and 76. For this BPM $p_H - p_C = -0.5$ which is close to the limit for anti-proton reliability. However the data outside of stores 56 to 76 are very stable; moreover the data for VB14, VC49 and HB17 are also very stable even though those BPMs are even closer to the reliability limit for anti-proton information. Therefore the observed steps in the HD12 data probably do not arise from normal fluctuations of the cancellation coefficients; they indicate some other effect.
- The other two BPMs that were initially classified as outliers, VC49 and HB17 (magenta), look very much like the BPMs from the tail of the main body (green). I conclude that they should not be considered not as outliers but rather as part of the main body of data.

BPM	Store Number	Time Stamp	$\bar{p}_H - p_C$ (mm)
VA14	29	07/27/05 06:27	3.666
	30	07/28/05 11:06	2.056
HD12	55	09/08/05 13:38	0.990
	56	09/09/05 09:19	0.612
	57	09/10/05 23:56	1.483
	61	09/16/05 02:15	1.456
	62	09/17/05 14:23	0.551
	75	10/05/05 22:11	0.375
	76	10/08/05 04:36	1.242

Table 1: Stores before and after each step in the VA14 and HD12 anti-proton helix size. The second column gives the store number within this study. The third column gives the time stamp on the data file, which is typically an hour after the start of the store. The last column gives the measured size of the anti-proton helix, in mm.

Table 1 identifies the stores just before and after each step in the data for VA14 and HD12. I have looked back through the project email list and I have not found any entries that would explain a jump in the measured helix size at these times. Luciano and Marv have also checked their records and they did not find anything that would explain these jumps.

The upper plot in Figure 4 shows the size of the proton helix, $p_H - p_C$, at VA14 and the second plot from the top repeats the VA14 anti-proton data from the Figure 3. The second plot from the bottom shows the size of the proton helix at HD12 and the bottom plot repeats the HD12 anti-proton data from Figure 3. For both BPMs the proton data is completely stable at the times of the structure in the anti-proton data.

Figure 5 repeats the plot of $\bar{p}_H - p_C$ vs store number for VA14 and adds plots of $\bar{p}_H - p_C$ vs store number for four other nearby BPMs, two on each side of VA14. None of the four additional BPMs have any structures that correspond to the step seen in the VA14 data.

Figure 6 repeats the plot of $\bar{p}_H - p_C$ vs store number for HD12 and adds plots of $\bar{p}_H - p_C$ vs store number for five other nearby BPMs, two on one side of HD12 and three on the other. None of the five additional BPMs have any structures that correspond to the step seen in the HD12 data.

Taken together, the last three figures strongly suggest that the steps seen in the VA14 and HD12 anti-proton data are instrumental artifacts.

5 Anti-Proton Stability vs Proton Helix Size

In the discussion of Figure 3 it was noted that several of the BPMs in the tail or in the outliers, had proton helix sizes close to the limit for reliable anti-proton

data, $|p_H - p_C| > 0.25$ mm. To investigate this further, Figure 7 shows a scatter plot of $R_{\bar{p}}$ plotted against the mean value of the proton helix size, $|p_H - p_C|$; the mean is taken by averaging all of the stores included in the study. The handful of points with large $R_{\bar{p}}$ do indeed cluster at small values of $|p_H - p_C|$. But there are no other significant trends in the data; there are some hints but nothing significant. Had the points with $|p_H - p_C| < 0.25$ mm been plotted, most of them would have been off-scale high near $R_{\bar{p}}$ of several mm. From Figure 7 one can conclude that a subset of the BPMs with $0.25 < |p_H - p_C| < 1.0$ mm have anti-proton information of less than optimal quality, but many other BPMs in this range have excellent anti-proton information. Even for those with less than optimal information, the data is still very usable.

6 Summary and Conclusions

This note has shown that both the proton and anti-proton helix size measurements have excellent stability. The method used here sets an upper limit on the stability of $< 40 \mu\text{m}$ for a typical proton measurement, with a worst case of $< 80 \mu\text{m}$, and of $< 62 \mu\text{m}$ for a typical anti-proton measurement, with a worst case of $< 150 \mu\text{m}$. This does not prove that the system meets the stated long term stability requirement of $< 20 \mu\text{m}$ but it does demonstrate what the system can do.

There are, however, two of 217 BPMs for which there are unexplained jumps in the anti-proton helix size. Further investigation suggests that the jumps are likely to be instrumental artifacts. As yet there is no explanation for these.

This note also looked for correlations between $R_{\bar{p}}$ and $|p_H - p_C|$. The main body of the data has no significant correlation but the handful of points with the largest values of $R_{\bar{p}}$ do cluster at small values of $|p_H - p_C|$.

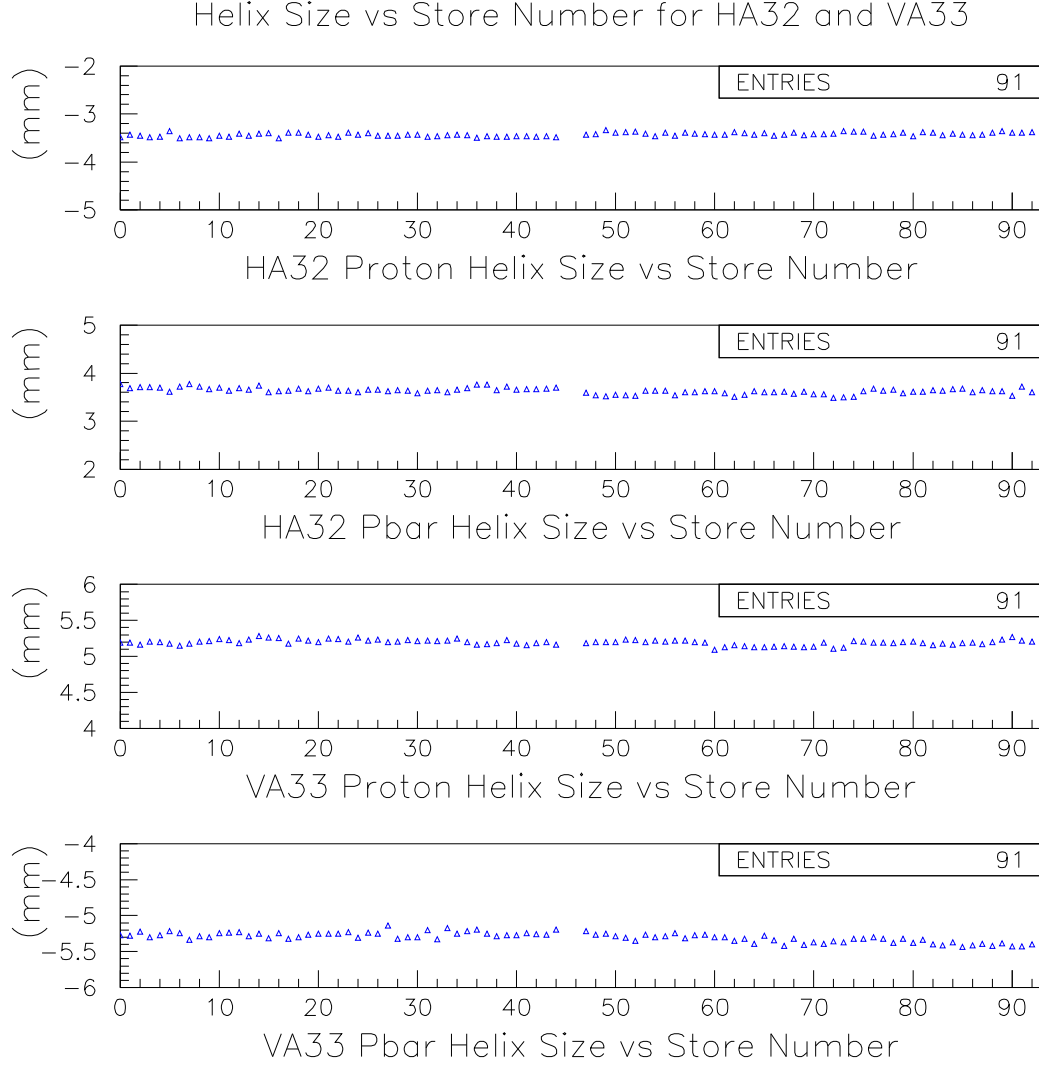


Figure 1: Measurements of the helix size plotted against time; the horizontal axis is store number within this study and there is one data point per store. The upper plot shows the size of the proton helix, $p_H - p_C$, at HA32, and the second plot the size of the anti-proton helix, $\bar{p}_H - p_C$, at HA32; the last two plots show the same quantities for VA33. These data are typical of the 217 BPMs in the study. A few points are missing for reasons discussed in the text.

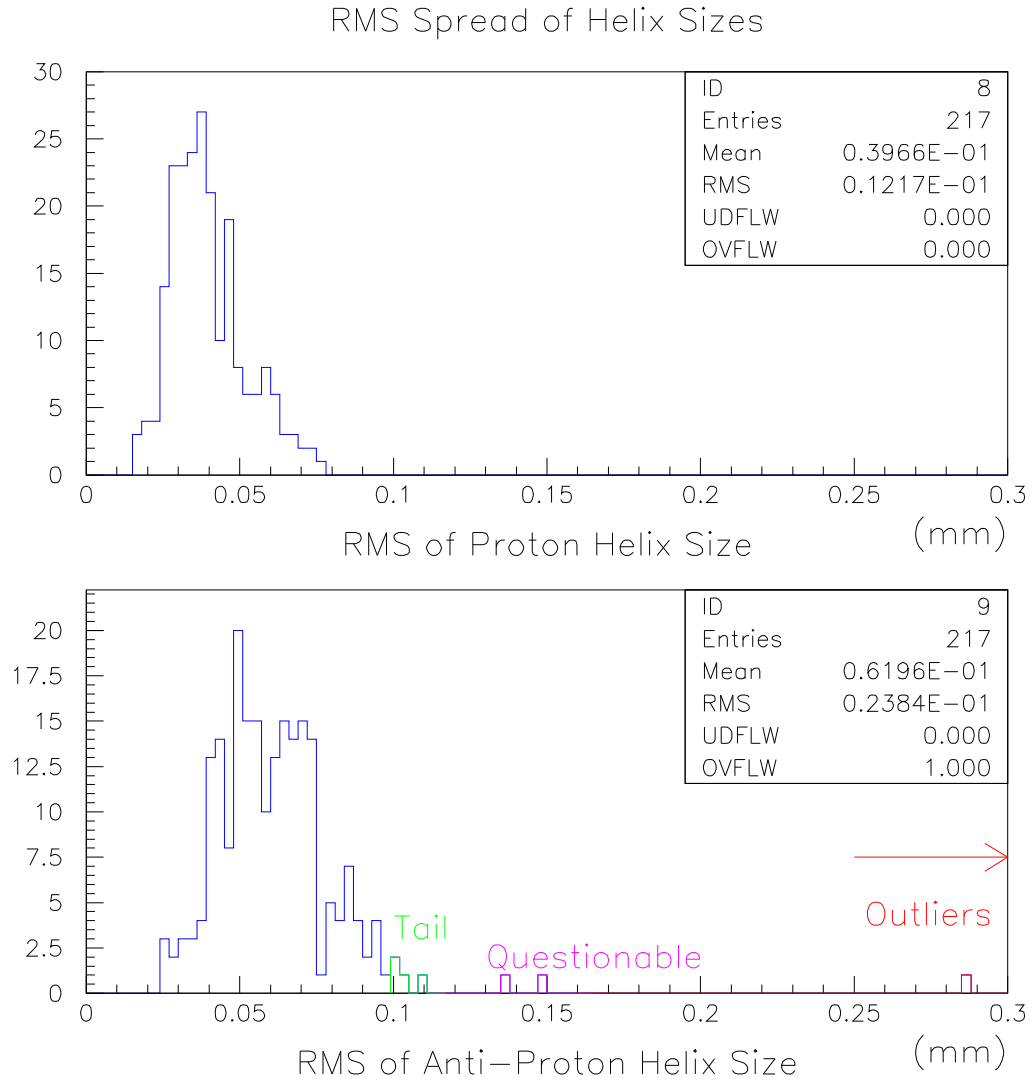


Figure 2: The upper plot shows a histogram of the RMS spread of $p_H - p_C$, the proton helix size, as measured at each of 217 BPMS. There is one entry per BPM. The lower plot shows a histogram of the RMS spread of $\bar{p}_H - p_C$, the anti-proton helix size, as measured at the same 217 BPMS. Eight entries in the lower plot have been selected for further investigation, the tail of the main distribution, shown in green, two outliers, shown in red, including one overflow, and two questionable points, shown in magenta, that might or might not be outliers.

Anti-Proton Helix Size for BPMs with $R_{\text{pbar}} > 0.1$

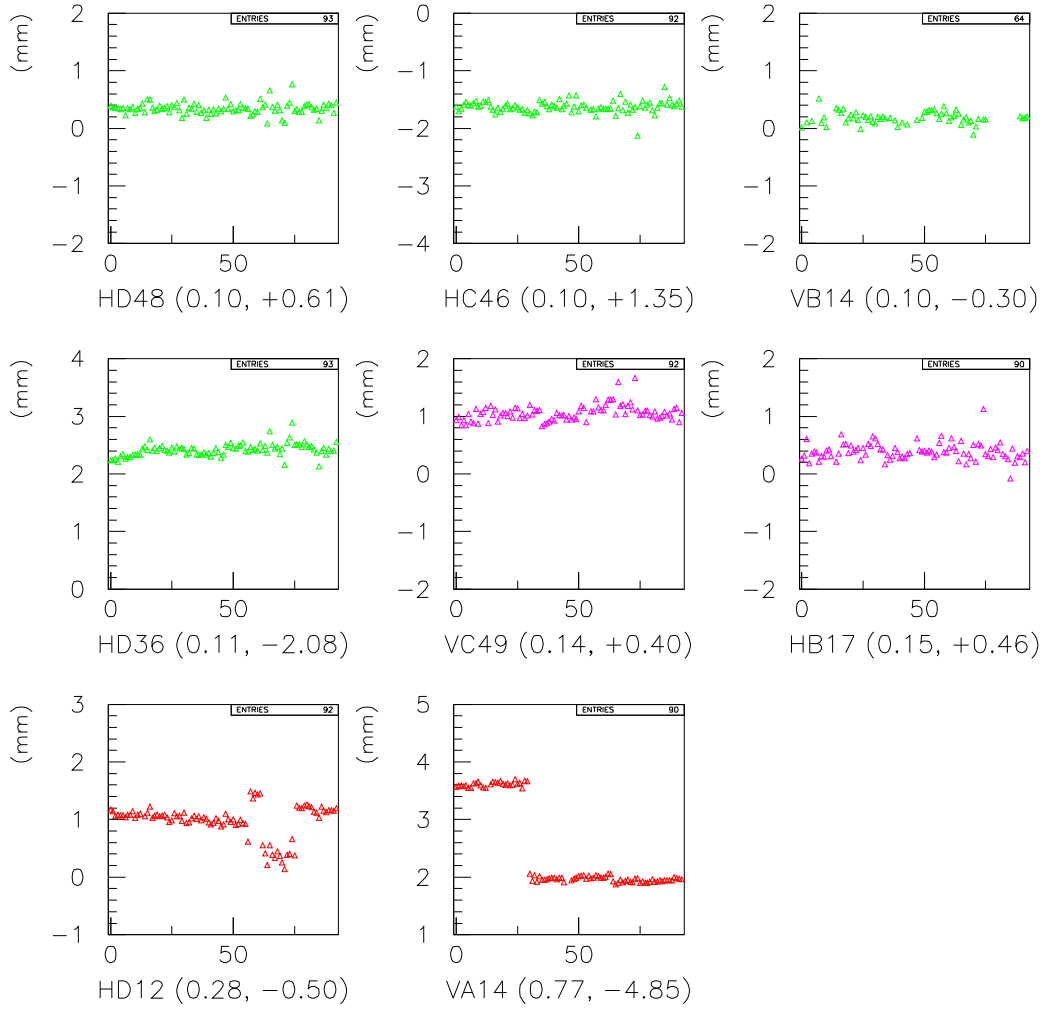


Figure 3: Anti-proton helix size vs store number for the four BPMs initially classified as outliers (red and magenta) and for four reference BPMs (green) from the tail of the main body of the data. The plots are ordered in increasing order of R_{pbar} , the first of the pair of numbers in each title. The second number in each pair is the size of the proton helix for that BPM. There is definite structure in the two outliers, HD12 and VA14, while the questionable BPMs (magenta) are consistent with being part of the main body of the data (green). The dates and times of the steps in the VA14 and HD12 data are given in Table 1.

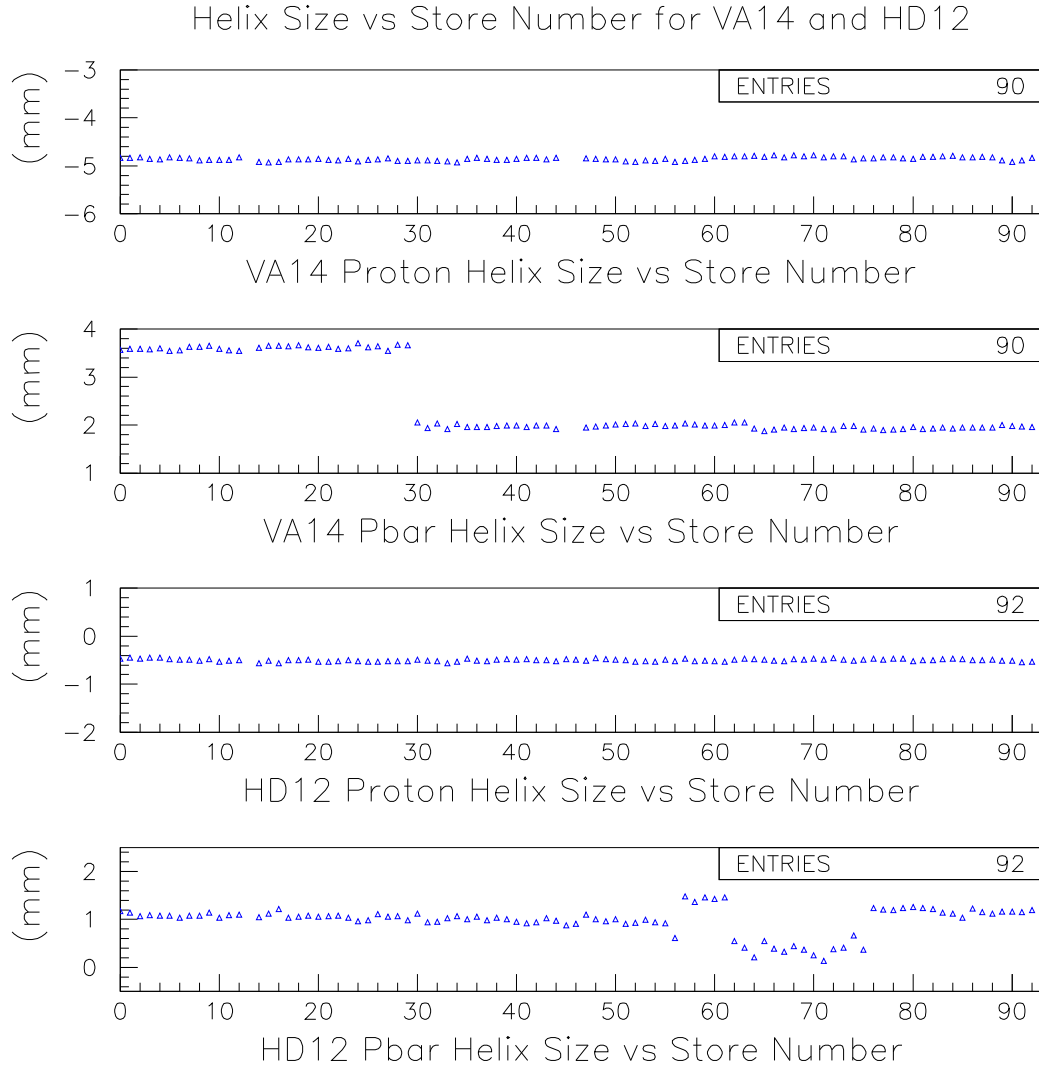


Figure 4: Time series of helix size vs store number for the two BPMs with definite structure in the previous figure. In both cases, the structure is present only in the anti-proton data, not the proton data.

Anti-Proton Helix Size vs Store Number for BPMs near VA14

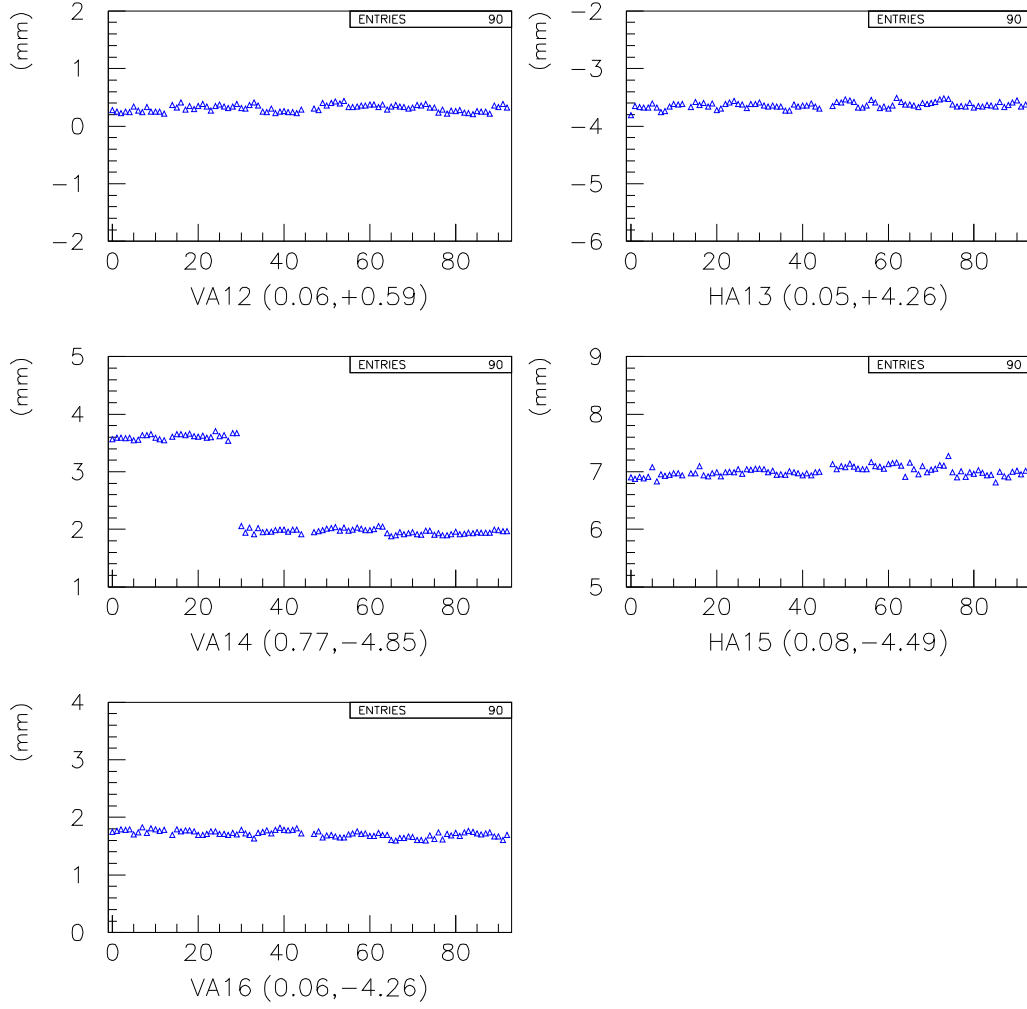


Figure 5: Time series of anti-proton helix size vs store number for VA14 and two BPMs on either side. The step seen in the VA14 data is not present in any of the other BPMs. The numbers in () in the plot titles are $(R_{\bar{p}}, p_H - p_C)$, where the second number was averaged over all stores in the study. The dates and times of the steps in the VA14 data are given in the Table 1.

Anti-Proton Helix Size vs Store Number for BPMs near HD12

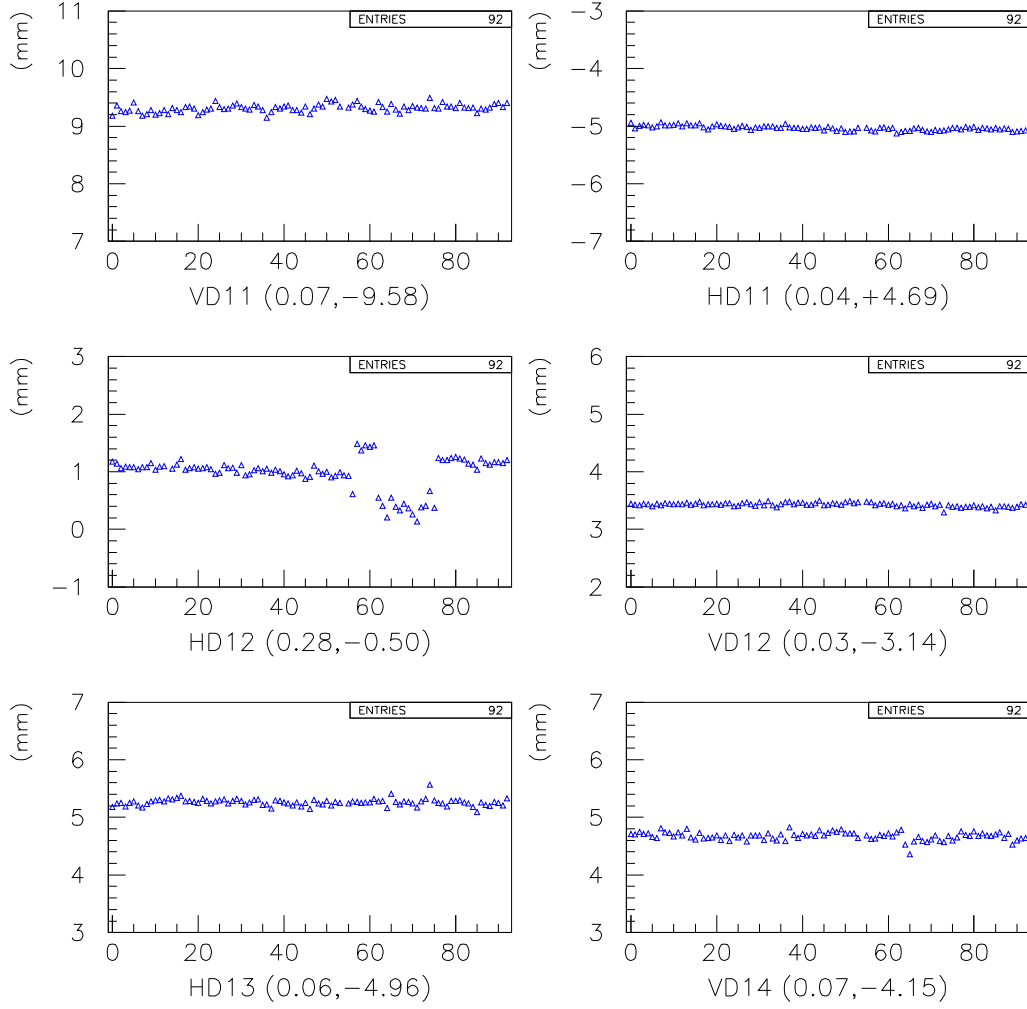


Figure 6: Time series of anti-proton helix size vs store number for HD12 and a few BPMs on either side. The step seen in the HD12 data is not present in any of the other BPMs. The numbers in () in the plot titles are $(R_{\bar{p}}, p_H - p_C)$, where the second number was averaged over all stores in the study. The dates and times of the steps in the HD12 data are given in the Table 1.

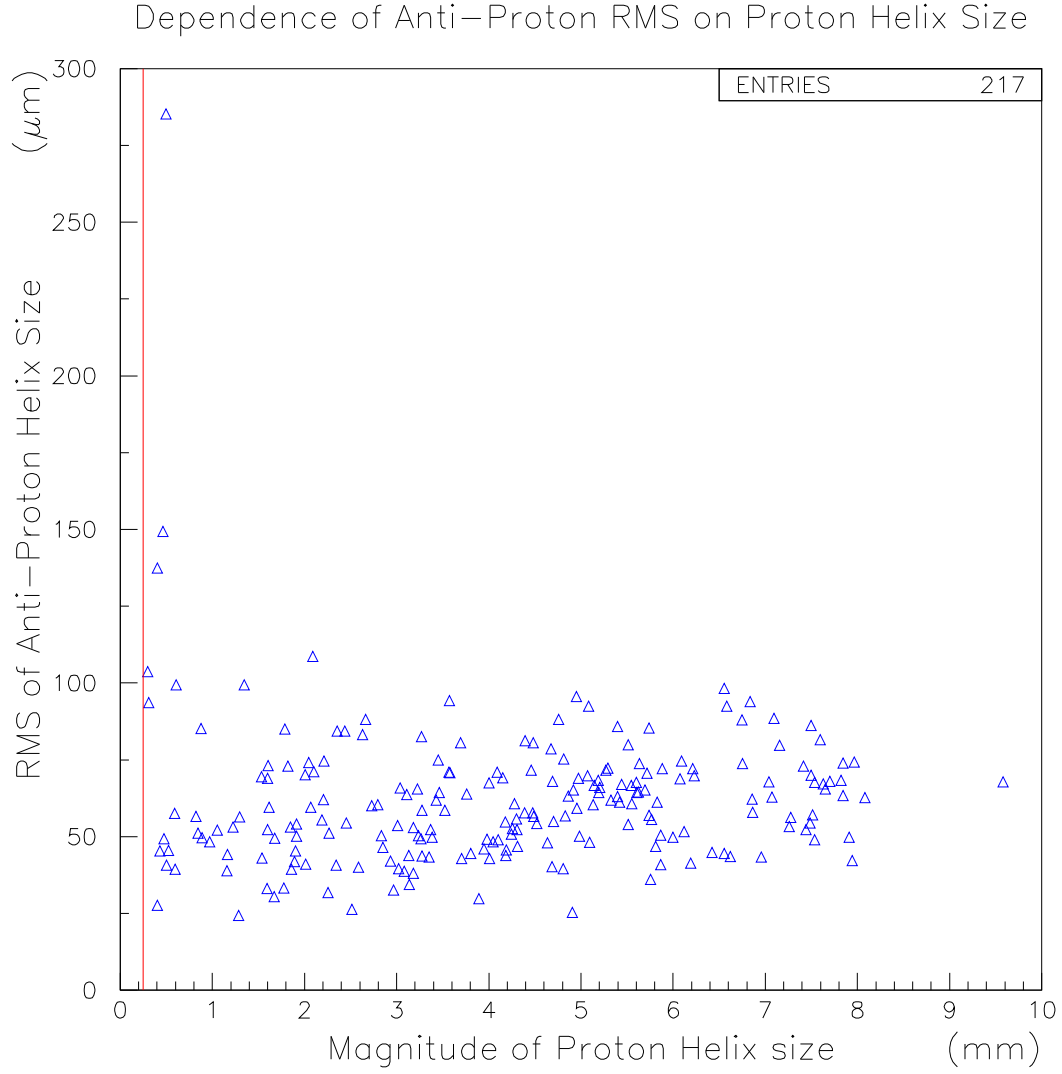


Figure 7: A scatter plot of $R_{\bar{p}}$ vs $|p_H - p_C|$. The vertical red line marks the cut below which the anti-proton data are rejected as unreliable. The points with large values of $R_{\bar{p}}$ cluster at small values of $|p_H - p_C|$.